



New chamber stapes prosthesis: Effect of ionizing radiation on material and functional properties

Monika Kwacz ,
Jarosław Sadło ,
Marta Walo

Abstract. New chamber stapes prosthesis (ChSP) is a middle-ear prosthesis intended for use in ear surgery for restoring the patient's middle ear function. As the prosthesis is an implantable medical device, it must be sterilized before use. However, possible alterations in the material and the functional properties following the sterilization process can influence the safety aspects while using the prosthesis. The purpose of this paper was to determine the effects of ionizing radiation (IR) on the physicochemical and biological properties of the new chamber prosthesis by utilizing EPR spectroscopy, mechanical testing, and cytotoxicity studies. Our research shows that the radiation treatment increases the hardness and the elastic modulus of the polymer, decreases the stiffness of the prosthesis membrane, and does not cause chemical changes in the polymers that may result in cytotoxicity. Furthermore, new ChSPs were successfully tested in preclinical *in vitro* tests. The test results justify the undertaking of further work, including *in vivo* biocompatibility tests and clinical trials, which would eventually lead to the increased use of the prosthesis in clinical practice.

Keywords: Chamber stapes prosthesis • Cytotoxicity • EPR spectroscopy • Mechanical testing • Radiation sterilization

Introduction

New chamber stapes prosthesis (ChSP) [1, 2] is a middle-ear prosthesis device designed for application in ear surgery for restoring the patient's middle-ear function. Stapes prostheses are commonly implanted in patients suffering from conductive or mixed hearing loss that is caused by stapes otosclerosis. In otosclerosis [3], the mobility of the stapes is significantly reduced by the abnormal bone growth in the oval window niche, or by the stiffening of the stapes annular ligament. Due to its limited ability to self-repair, otosclerosis needs to be mostly treated by stapedotomy surgery [4].

Stapedotomy with a piston prosthesis is the standard procedure, as it is minimally invasive, relatively safe, and efficient [5, 6]. During surgery, the stapes superstructure is removed, a small hole is made in the stapes footplate, the piston of the prosthesis is introduced into the hole, and the prosthesis is attached to the incus or malleus. Auditory outcomes are generally perceived as good but only for low and medium frequencies (0.5–3 kHz), and a large number of patients report a lack of satisfactory results for higher frequencies [7, 8]. Moreover, the piston prosthesis malfunction (displacement from a small

M. Kwacz
Institute of Micromechanics and Photonics
Faculty of Mechatronics
Warsaw University of Technology
św. Andrzeja Boboli 8 St., 02-525 Warsaw, Poland

J. Sadło, M. Walo
Centre for Radiation Research and Technology
Institute of Nuclear Chemistry and Technology
Dorodna 16 St., 03-195 Warsaw, Poland
E-mail: m.walo@ichtj.waw.pl

Received: 10 March 2024
Accepted: 24 May 2024

hole or of incus, immobilization by adhesion or fibrous tissue, necrosis or erosion of the long process) causes the reappearance of conductive hearing loss and requires revision stapes surgery [9]. Following revision stapedotomy, the hearing results are less satisfactory than after the primary operation, and the incidence of vertigo, high-frequency tinnitus, and/or sensorineural hearing loss are the most probable complications [10, 11].

The ChSP allows overcoming the unsatisfactory hearing results and malfunction observed occurring following classical piston stapedotomy or re-stapedotomy [2]. Furthermore, for the ChSP, the surgical procedure remains the same as for the piston stapedotomy. The ChSP (Fig. 1) mimics the natural ear and consists of: (1) a chamber mimicking the vestibule, (2) a flexible membrane mimicking the stapes annular ligament, and (3) a rigid plate mimicking the stapes. Both the chamber and the rigid plate are designed to be made of UV curable polymer and the membrane of a thin poly(dimethylsiloxane) (PDMS) film. To restore normal hearing after the ChSP stapedotomy, the stiffness of the flexible membrane should be close to the stiffness of the normal stapes annular ligament (~ 120 N/m, [12]).

As the ChSP is an implantable medical device (class III), it must be sterilized before use [13]. Efficient sterilization is crucial to minimizing the incidence of medical device-related infections, which are a major concern in health care [14]. For implants, ISO 14630:2013 [15] requires a sterility assurance level (SAL) of 10^{-6} , which is equivalent to the probability of one in a million spores surviving the sterilization process [16]. This level can be achieved using a number of physical and chemical methods [17, 18] such as high temperature exposure (e.g., moist or dry heat sterilization), chemical (e.g., ethylene oxide, formaldehyde), or chemical plasma exposure (H_2O_2), and ionizing radiation (IR). However, the sterilization methods employed may lead to adverse changes in the physical, mechanical and chemical properties of the materials, eventually allowing the formation of toxic residues, and may also change the functional properties of the whole device [19–21]. Steam sterilization can lead to hydrolysis, softening, and degradation of the polymers due to the high temperature, pressure, and humidity [17]. IR (gamma and electron beam [EB]) initiates the formation of very reactive

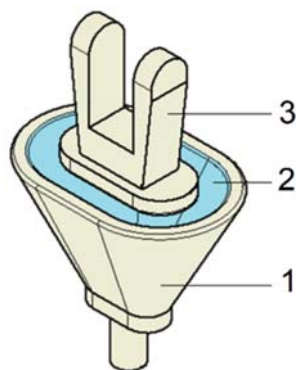


Fig. 1. Chamber stapes prosthesis. 1 – chamber, 2 – flexible membrane, 3 – rigid plate as a function of applied field.

species in polymers (free neutral radicals, cationic and anionic ions, excited molecules), leading to the changes in the physicochemical properties of the irradiated materials. This results in cross-linking, chain scission, or oxidation [22]. Furthermore, both steam and IR may deform and cause yellowing of the polymeric materials. For these reasons, the effects of sterilization on the properties of the ChSP must be carefully examined.

The choice of the most suitable sterilization method for the ChSP depends on the nature and characteristics of each specific material used for the production of the prosthesis. Since the polymers to be used are sensitive to most of the sterilizing agents, including heat, ethylene oxide, formaldehyde and also due to the risk of membrane damage, radiation sterilization of the ChSP is foreseen to be the technique of choice. The advantages of radiation technique comprise high penetration, high efficiency in destroying microorganisms, good assurance of device sterility, no leaving behind chemical residues, the ability of operating at low temperatures, and the possibility of using the materials immediately after the sterilization process [23]. However, possible alterations in the material and the functional properties after irradiation can affect the safe use of the prosthesis. Therefore, comprehensive chemical characterization and analysis of the final sterilized ChSP are important aspects of the biological evaluation according to the ISO 10993-18 standard [24].

Radiation sterilization is generally used for the sterilization of pharmaceutical formulations and medical devices, such as syringes, needles, and cannulas [25]. For this technique, the reference sterilization conditions refer to an absorbed dose of 25 kGy, but other levels can be employed provided that has been a validation process conducted [26].

The use of IR was successfully applied for the sterilization of many polymeric biomaterials including nondegradable polymers and biodegradable ones. For example, Zhao *et al.* [27] demonstrated that EB can be applied for the sterilization of polymer blends of polyactive (PLA), poly(butylene adipate-co-terephthalate) (PBAT), and their blends, where PLA can be used for transparent medical devices such as the barrel of syringes or microfluidic chips, while PBAT and PLA/PBAT blends for other non-transparent medical packaging applications. Other studies conducted by Munker *et al.* [19] confirmed that the gamma ray sterilization appears to be a suitable technique when used to sterilize poly(methyl methacrylate) PMMA-based personalized medical devices. Radiation sterilization has also been successfully used for the sterilization of bone grafts [28], dental grafts [29], and collagen scaffolds [30].

The objective of this study was to determine the effects of radiation sterilization on the chemical, biological, mechanical, and functional properties of a new ChSP. We intend to confirm that the radiation sterilization is an appropriate method and ensures safe and effective functioning of the ChSP. An additional objective was to provide data for the future optimization of some important ChSP design parameters.

Methods

Materials

The ChSPs were made of two components: (1) Silpuran® film 2030 (Wacker Chemie AG, München, Germany, www.wacker.com) and (2) DS3000 (DWS srl, Thiene, Italy, www.dwssystem.com).

Silpuran® is a chemically stable and biocompatible (USP Class VI) cross-linked silicone rubber (PDMS). We have used the 50 µm, 100 µm, and 200 µm films to make up the flexible membrane for the ChSP samples.

DS3000 is a photosensitive and biocompatible (USP Class I) liquid polymer. We have polymerized this polymer using a self-made 3D printer (PW-IMIF, Warsaw, Poland) working using the digital light processing (DLP) technology. The PW-IMIF printer is equipped with a high brightness modular DLP-based projector (PRO4500, Wintech Digital System Technology Corp., San Marcos, CA, USA) that consists of a light engine (UV light, 385 + 10 nm) and a driver board. For all the samples, the polymerization process was performed in the same environment and according to the same validated methodology.

The objective of our research was to study the radiation stability and the functionality of the ChSP. However, in order to facilitate the interpretation of some research results, the component materials were also analyzed, i.e., the Silpuran membrane (with various thicknesses) and the polymerized DS3000 polymer.

EB sterilization

The sterilization process was carried out at the Radiation Sterilization Station for Medical Devices and Allografts of the Institute of Nuclear Chemistry and Technology (Warsaw, Poland). EB sterilization in the presence of air, in vacuum, and with deionized water was performed at room temperature using a 10 MeV EB generated in a linear electron accelerator Elektronika 10/10 to a dose of 25 kGy. The absorbed dose was controlled using polystyrene calorimeters from RISØ High Dose Reference Laboratory.

Gamma sterilization

Gamma sterilization in the presence of air at room temperature was performed in the Gamma Chamber GC5000 cobalt source (BRIT, India) to a dose of 25 kGy at a dose rate of about 2.8 kGy/h. The absorbed dose was controlled with an alanine dosimeter according to ISO/ASTM 51607:2013(E) Standard Practice for Use of an Alanine-EPR Dosimetry System.

EPR spectroscopy

Radiation-generated paramagnetic species in the Silpuran® film 2030 (thickness 200 µm), DS3000,

and whole ChSPs were tested using the electron paramagnetic resonance (EPR) method. In addition, two ChSP samples irradiated under different conditions, such as (1) immersed in deionized water and (2) closed in a vacuum, were also studied to investigate the influence of irradiation conditions on the tested materials.

Before the EPR measurements, the samples were irradiated in the gamma source (GC5000) and in the electron accelerator (Elektronika 10/10) with a dose of 25 kGy at room temperature with air access. After irradiation, the samples were placed into suprasil tubes, and the EPR spectra were recorded at room temperature using an EMXplus Bruker X-band spectrometer equipped with a nitrogen cryostat having an ER4131VT temperature controller and a cylindrical resonant cavity with high sensitivity. The following parameters were applied: sweep width to 60.0 mT, microwave power 1 mW, modulation amplitude 0.1 mT, conversion time 15 ms, and time constant 1.28 ms. The number of scans was adjusted according to the intensity of the experimental signals. The radicals generated in the irradiated materials were monitored and identified using WinEPR (Bruker, Germany) software.

Mechanical testing

Hardness and the elastic modulus for the polymerized DS3000 in the cuboids form (5 mm × 2 mm × 2 mm) before and after the EB sterilization were measured using a Micro-Indentation Tester (MHT, CSM Instruments, Needham, MA, USA) equipped with a calibrated Vickers indenter tip. The tests were performed in accordance with recommendations of the ISO 14577 standard [31]. The trapezoidal indentation load profile with a maximum force of 5 N, a 5 N/min loading and unloading rate, and a 2 s holding period have been set. For each sample, 10 indentations were carried out.

During the indentation, the force (F) and the indentation depth (d_c) were continuously monitored and a curve of force vs. depth ($F-d_c$) was recorded. Hardness and elastic modulus were calculated using the Oliver and Pharr method [32, 33]:

$$(1) \quad H = \frac{F_{\max}(d_{\max})}{A(d_c)}$$

Stiffness of the Silpuran membrane of the 50 µm, 100 µm, and 200 µm thicknesses before and after the EB sterilization was measured using an AFM NT-206 system (Microtestmachines Ltd., Gomel, Belarus) (Fig. 2). The system consists of a scanning unit, a controller, and software for AFM-data processing, visualization, and analysis. The measurement procedure was the same as described in Ref. [12]. Briefly, the AFM was equipped with a cantilever made in the Institute of Micromechanics and Photonics at the Warsaw University of Technology. The rectangular cantilever beam was etched out of a thin (60 µm) beryllium copper plate (Alloy Brush 190 CUBE2, BE 1.8%, Co+Ni 0.3%, Laminaries Matthey SA, La Neuveville, Switzerland) with a polished reflective

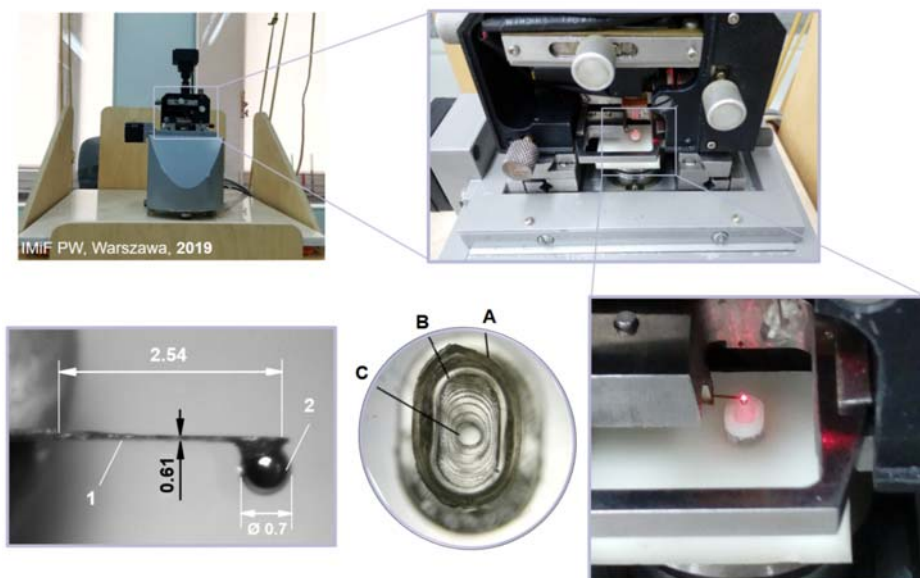


Fig. 2. Measurement of stiffness of the chamber stapes prosthesis membrane. Top left – the AFM system; top right – the scanning unit of the AFM; bottom left – the cantilever; bottom middle – ChSP; bottom right – the cantilever mounted in the holder and the sample placed on the AFM Table 1 – cantilever beam, 2 – tip of the cantilever. A – a ring for attaching the membrane to the chamber, B – the chamber, C – the membrane.

upper surface. As a tip of the cantilever, a stainless-steel bearing ball with a diameter of 0.7 mm was used. The real spring constant (k_c) of the cantilever was measured using the calibration method described by Ekwińska and Rymuza [34]. Based on the calibration curves, the k_c value was 200.0 N/m. After the calibration, the cantilever was mounted in the cantilever holder of the measuring head. The ChSP sample was placed on the AFM table and moved to contact with the cantilever tip. Then, the force-distance ($F-d$) curves were recorded using the closed-loop force mode with a maximum displacement of ~450 nm applied at a rate of about 100 nm/s. For each sample, 40 measurements were done, and the stiffness of the membrane was determined based on the recorded $F-d$ curves.

ICP-MS

The ICP-MS was used to determine the content of toxic elements in the main component of ChSP, i.e., sterilized DS3000. The analysis was performed using an Agilent 7800 ICP-MS spectrometer (Agilent Technologies Inc., Santa Clara, CA, USA) with MassHunter 4.2 Software and Pre-set Methods. After ashing the sample, the residue was dissolved in a 1% nitric acid solution and introduced into the nebulizer. The content of arsenic (As), selenium (Se), cadmium (Cd), antimony (Sb), mercury (Hg), and thallium (Tl) was tested. The limits of quantification (LOQ) for these elements are listed in Table 1.

In vitro-cytotoxicity test

The cytotoxicity of the ChSP was tested at the National Medicines Institute (Warsaw, Poland) in accordance with recommendations of the ISO 10993-5 standard [35]. The methods used were covered by the PCA accreditation (certificate no. AB 774, Polish Centre for Accreditation). Mouse fibroblasts, a clone of strain L (NCTC clone 929, ATCC No CCL-1, American Type Culture Collection, Rockville, MD), were trypsinized and resuspended in Eagle's minimum essential medium with glutamine (MEM, Biowest, batch no. 9918369L0415) supplemented with 10% fetal bovine serum (FBS, Biowest, batch no. S16337S1810), 1% antibiotics solution (amphotericin B, penicillin, and streptomycin; Biowest, batch no. S17660L0010). The cells were routinely grown in the 96-well microliter plates in a humidified atmosphere (5% CO₂, 95% air) at 37°C. After 24 h, the cells were exposed (48 h) to the extract of the ChSP sample. The extract was prepared under sterile conditions by incubating the sample suspension (0.2 g/mL) in MEM with 10% FBS at 37°C for 24 h. The cytotoxic effect induced by the ChSP extract was evaluated visually (qualitative evaluation) by microscopic observation using a cytotoxicity scale according to ISO 10993-5 [36], i.e., 0 (none): discrete intracytoplasmic granules, no cell lysis; 1 (slight): not >20% of the cells are round, loosely attached, and without intracytoplasmic granules; occasional lysed cells present; 2 (mild): not >50% of the cells are round and devoid of intracytoplasmic granules; no extensive cell lysis and empty

Table 1. Limits of quantification (LOQ) for the determined elements

Element	As	Sb	Se	Hg	Cd	Tl
LOQ (µg/kg)	0.0005	0.0008	0.03	0.04	0.0002	0.008

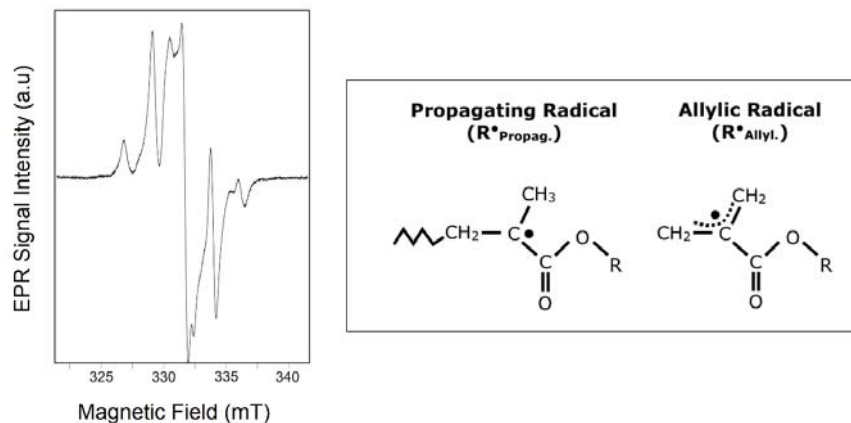


Fig. 3. Left – EPR spectrum of polymerized DS3000 recorded at room temperature after the irradiation with a dose of 25 kGy in the Elektronika 10/10 electron accelerator. Right – the propagating and allylic radical in dental resin.

areas between cells; 3 (moderate): not >70% of the cell layers contain rounded cells or are lysed; and 4 (severe): nearly complete destruction of the cell layers. The achievement of a numerical grade >2 is considered a cytotoxic effect.

Results and discussion

The ChSP is a new implantable medical device whose effectiveness has been confirmed in preclinical tests [2]. The purpose of the tests was to check the sound transmission characteristics in human cadaver temporal bone specimens. Therefore, non-sterile prostheses have been used during the implantation procedure. However, for planned clinical trials, sterile prototypes have to be prepared. These prototypes should ensure both the effectiveness and safety of use. Thus, choosing the proper biocompatible materials and the appropriate sterilization methods is particularly important. Below, we present the results of the studies for ChSP irradiated with EBs and gamma rays, in order to check whether radiation sterilization has an impact on the physicochemical properties of this type of biomaterial.

EPR spectroscopy

The EPR spectroscopy is a very sensitive method that allows to detect and identify paramagnetic intermediates in the irradiated materials. Knowledge of the radical processes occurring in irradiated polymers is crucial because IR may affect the physicochemical properties of the sterilized product [36–38]. The result of radiation sterilization of the polymers can be influenced by the irradiation conditions (inert gas atmosphere, air, vacuum), temperature, selection of the irradiation source, absorbed dose, and dose rate.

For the Silpuran membrane (PDMS), both irradiated in the electron accelerator and gamma source, no EPR signals were recorded. This result indicates that radicals generated by radiation in the cross-linked silicone rubber are highly unstable at room temperature.

In the case of the polymerized DS3000, the EPR spectrum (Fig. 3, left) recorded at room temperature

is complex and consists of at least two signals. The first is a pentet with splitting of $A = 2.3$ mT and the second signal is difficult to identify due to signal overlapping. Lamblin *et al.* [39] observed a similar spectrum in dental resin and assigned it to two radicals: (1) the allylic radical and (2) the propagating radical giving nine broader lines (Fig. 3, right).

The intensity of EPR signals of DS3000 decreases rapidly as shown in Fig. 4 that presents the EPR spectra of the sample irradiated in the gamma source and recorded immediately after irradiation and after 24 h. The signals from the allyl radical and the propagating radical disappear, while the low-intensity doublet remains, which is no longer subject to further changes.

The signals recorded in the ChSP sample irradiated with an EB behave differently for samples placed in deionized water and in vacuum (Fig. 5). The sample irradiated in deionized water was immediately after irradiation dried with tissue paper and

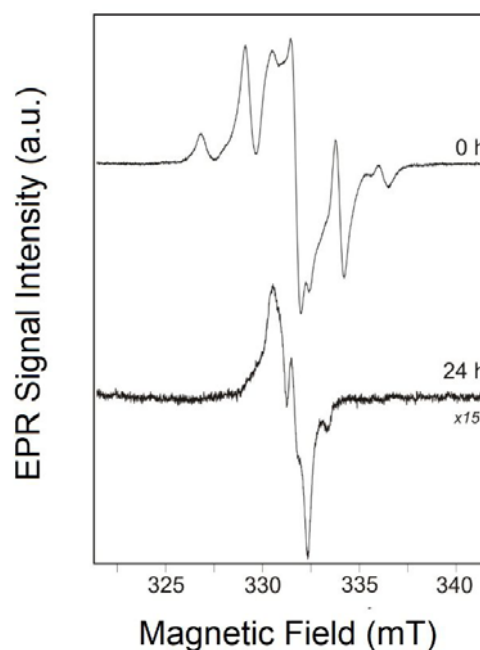


Fig. 4. EPR spectra of the polymerized DS3000 irradiated in the GC5000 gamma source with a dose of 25 kGy recorded immediately after irradiation and after 24 h.

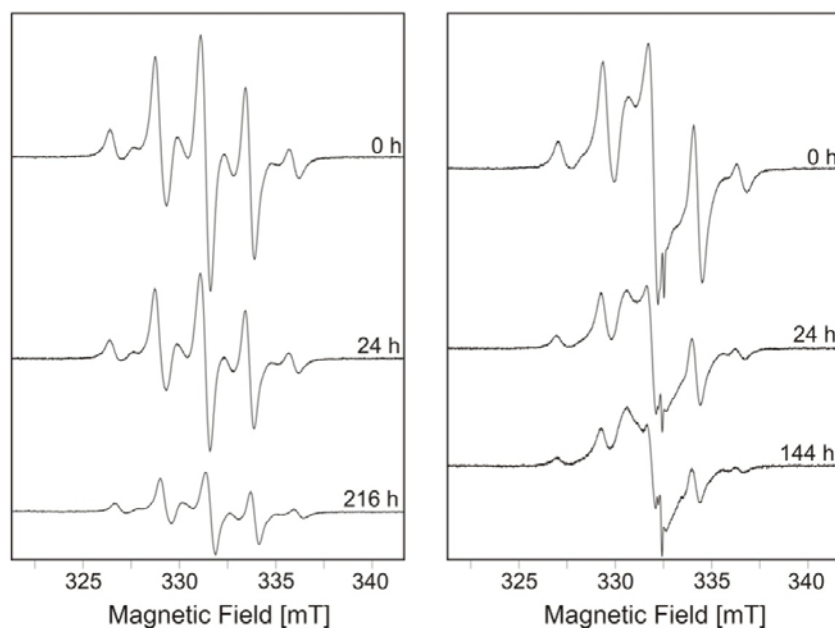


Fig. 5. The EPR spectra of the chamber stapes prosthesis irradiated in the Elektronika 10/10 electron accelerator recorded directly, 24 h and 216/144 h after irradiation. Left – the sample irradiated in deionized water. Right – the sample irradiated in vacuum.

placed in a measuring tube. From that moment, it was in contact with the air. The sample irradiated in vacuum remained in the quartz tube all the time. In both cases, the disappearance of signals occurs much more slowly, and all the time, there were signals of radicals as identified by Lamblin *et al.* [39]. In the sample irradiated in water, in addition to the pentet derived from the allyl radical, a series of weaker lines attributed to the propagating radical can be seen, while there is no signal of $g = 2.010$, occurring in samples irradiated under other conditions.

Based on the EPR spectra recorded for the polymerized DS3000 and ChSP samples irradiated under different conditions, the relative relationship of EPR intensity as a function of time after irradiation, defined as a measure of the double integral of the entire

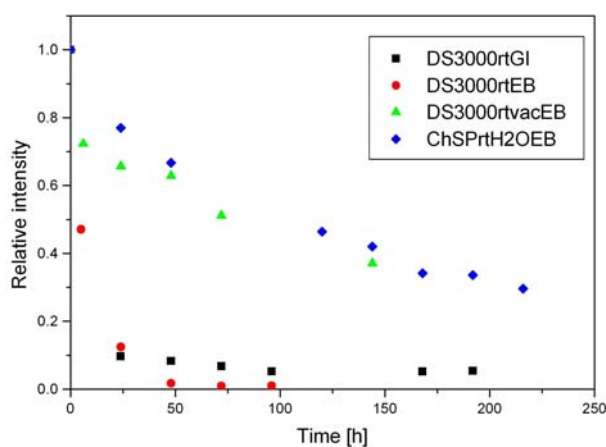


Fig. 6. Relative contributions of the EPR signal intensity for the DS3000 and chamber stapes prosthesis samples after irradiation under different conditions as a function of time. The spectra were recorded at a microwave power of 1 mW. GI, gamma; EB, electron beam; rt, room temperature; vac, vacuum; H₂O, deionized water.

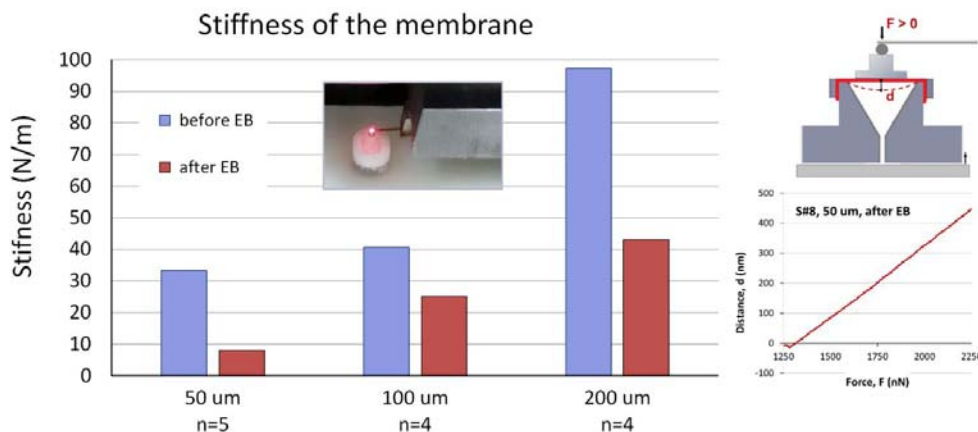
EPR spectrum, was analyzed. Figure 6 shows that the disappearance of the total population of radicals is similar for the DS3000 sample irradiated with air access when the radicals disappear quickly, and similar for the samples irradiated without air access (vacuum, deionized water) when the radicals decay much more slowly. It can be hypothesized that the oxygen participates in the reaction causing radicals decay. However, the explanation of this hypothesis requires additional tests to be performed.

Mechanical tests

The chamber and the plate of the ChSP are designed to be made of the DS3000 polymerized by UV light (385 nm) in the validated 3D printing process [40]. The same process was used to make the polymerized DS3000 samples. The samples were printed with an XY-resolution of 50 mm × 50 mm and a layer thickness of 50 mm. After printing, no surface smoothing was performed. It is well known that the surface roughness is an important issue for nanoindentation tests [41, 42]. This is because the real contact area (A) between the indenter and the sample surface is not only dependent on the material properties (hardness and elastic modulus) but also on the surface topography. Since the $A(d_c)$ is determined indirectly, the surface roughness of the polymerized DS3000 sample can cause errors in the $A(d_c)$ calculation. Consequently, this may lead to the incorrect determination of both the hardness (H), Eq. (1), and the elastic modulus (E). Two situations may arise during the measurement. One, when the indenter comes into contact with a peak, which results in greater stress, greater contact depth (d_c), and lower calculated hardness compared to the smooth surface indentation. The second, when the indenter comes into contact with a valley, which

Table 2. Hardness (H) and elastic modulus (E) of the polymerized DS3000 before and after irradiation (25 kGy)

DS3000	Hardness, H (MPa), $n = 4$		Elastic modulus, E (MPa), $n = 4$	
	Average value	1 SD	Average value	1 SD
Before EB	84.5	3.5	8500	1800
After EB	203.0	5.0	8900	400

**Fig. 7.** Stiffness (average value, before and after irradiation with 25 kGy) of the Silpuran membrane (thickness 50 μm , 100 μm , and 200 μm) attached to the chamber.

results in the opposite phenomenon, i.e., the A value is underestimated and consequently, the calculated hardness is overestimated.

The measurement results (Table 2) show that the EB sterilization (25 kGy) of polymerized DS3000 significantly increases the H value and slightly increases the E value. This may indicate the EB irradiation causes cross-linking that hardens the material [43]. Improvements of the mechanical properties of the DS3000 can positively influence by minimizing the risk of mechanical damage to both the chamber and the rigid plate during surgery.

The membrane stiffness in the ChSP (chambers with membrane of the 50 μm , 100 μm , and 200 μm thicknesses) was calculated based on the F - d curves recorded in the AFM measurements. The methodology of the calculation is described in detail in Ref. [12]. Figure 7 shows the stiffness of the membrane measured before and after the EB sterilization (25 kGy). Regardless of the thickness, irradiation significantly reduces the stiffness of the membrane.

The flexible membrane that closes the chamber is designed to be made of the biocompatible Silpuran[®] film 2030 (Wacker Chemie AG). The Silpuran[®] is a cross-linked silicone rubber, specially developed for the healthcare industry (USP class VI). The stiffness of the membrane depends on both the chamber geometry and the membrane thickness [44]. The stiffness can be increased by reducing the surface area and/or increasing the thickness of the membrane. These two parameters must be carefully chosen to ensure a final stiffness of about 120 N/m. Our measurement results (Fig. 7) show that the EB sterilization (25 kGy) significantly reduces the stiffness of the membrane. In the case of radiation-modified polydimethylsiloxane, cross-linking is the dominant process, and the decrease of stiffness is likely due to a degradation of the cross-linking points based on $(\text{Si-O})_n\text{-Si-(O-R)}_{4-n}$ units. The obtained results

showed that the Silpuran[®] film 2030 with a thickness of 100 μm or 200 μm , EB irradiated to a dose of 25 kGy, should not be used to make the membrane closing the chamber. The surface area should be determined by performing validation tests.

Due to the specific raster surface topography of the polymerized DS3000 samples (see the picture in Fig. 8), some indentations were omitted based on shape of the F - d_c unloading curves. For example, for the polymerized DS3000 sample after the EB sterilization, the slope (S) for the magenta slope lines varies from 2.19 mN/nm to 2.29 mN/nm, whereas the S for the black slope lines varies from 1.32 mN/nm to 1.71 mN/nm (mean value 1.48 mN/nm). This difference is due to a different location at which the

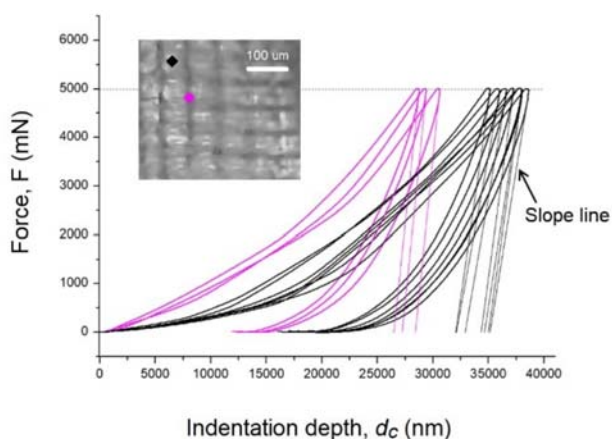
**Fig. 8.** Ten micro-indentation F - d_c curves (thick lines) for the polymerized DS3000 sample after the EB sterilization. The slope lines (thin lines) are added to the unloading curves to visualize the S parameter. Magenta F - d_c curves correspond to indentations on a slope or between the flat rasters (magenta diamond). Indentations were made with a trapezoidal loading scheme with maximum force of 5 N.

Table 3. Content of elements in the polymerized DS3000 sample (powered and sterilized)

Element	As	Sb	Se	Hg	Cd	Tl
(mg/kg)	<LOQ	<LOQ	<LOQ	<LOQ	<LOQ	<LOQ

LOQ, limit of quantification.

indentation was done. The raster topography of the sample surface implies that some indentations can occur on a slope or between the flat rasters (magenta diamond). This will result in the overestimation of the slope S . Therefore, the three $F-d_c$ curves (magenta) were omitted, and the H value was determined based on the seven $F-d_c$ curves (black).

ICP-MS

Table 3 summarizes the results of the ICP-MS analysis and shows the content of toxic elements in the polymerized and sterilized DS3000. The results show that no toxic element was introduced in hazardous quantities during the manufacturing process.

In vitro cytotoxicity

The DS3000 liquid raw material is probably a mixture of two monomers, i.e. triethylene glycol dimethacrylate (TEGDMA) and acrylic acid (AAc) with a certain amount of inhibitor. TEGDMA is commonly used as a photopolymerizable multifunctional monomer in the commercial dental restorative materials [45, 46]. It is recognized as a biocompatible material, because hydrophilic TEG chains show negligible toxicity and immunogenicity [47, 48]. Polyacrylic acid is also a well-known biocompatible polymer, which cross-links to form a network structure of PAAc. It can be used as a carrier in the drug release systems [49], as hydrogel scaffolds in tissue engineering applications [50, 51], or can be deposited on orthopedic implants to protect them from corrosion [52]. Since the TEGDMA is miscible with the AA over wide range dilutions [53], it is possible to obtain a biocompatible polymer with the mechanical properties suitable for the ChSP.

On the basis of the *in vitro*-cytotoxicity tests, only slight growth inhibition was observed and not >20% of the cells were round or showed changes in morphology in the cytotoxicity test done on the extract of the ChSP samples. Based on the qualitative morphological grading (Table 1 in ISO 10993-5 [25]), the cytotoxicity grade and the reactivity were determined as “1” and “slight”, respectively. As a result, the ChSPs were found to be noncytotoxic.

Conclusions

Our studies have shown that radiation sterilization (EB, 25 kGy) can be considered for sterilization of the ChSP. However, it should be borne in mind that irradiation changes the physicochemical properties of materials. On the one hand, the observed increase in hardness (from 84.5 MPa to 203 MPa) and Young's modulus (from 8.5 GPa to 8.9 GPa)

is a desirable phenomenon that improves the mechanical strength of the ChSP. On the other hand, the observed decrease in stiffness of the Silpuran membrane is an undesirable effect of IR since it reduces the effectiveness of the ChSP. In the next stage of research, it seems reasonable to irradiate ChSP with lower EB doses (5–20 kGy) in order to check the effect of radiation treatment on the mechanical properties of both the DS3000 polymer and the PDMS membrane. Perhaps using a lower dose would not cause such a significant change in the stiffness of the Silpuran membrane. An important conclusion is the lack of cytotoxicity of the DS3000 polymer, which is the main component of the ChSP (the cytotoxicity grade is “1” and the reactivity is “slight”, according to ISO 10993-5).

Acknowledgments. The authors would like to thank Pawel Grundland, MSc student, for preparing the samples for mechanical tests, Aleksandra Bek, BSc student, for preparing the samples for biological tests, and M. Milczarek for his help during the mechanical test.

ORCID

M. Kwacz  <https://orcid.org/0000-0002-6101-0435>
 J. Sadło  <https://orcid.org/0000-0002-6758-7032>
 M. Walo  <https://orcid.org/0000-0002-5115-6334>

References

- Gambin, W., Kwacz, M., & Mrówka, M. (2014). PL Patent 271562. UP RP.
- Kwacz, M., Solyga, M., Mrówka, M., & Kamieniecki, K. (2017). New chamber stapes prosthesis – A preliminary assessment of the functioning of the prototype. *PLOS One*, 12(5), e0178133. DOI: 10.1371/journal.pone.0178133.
- Quesnel, A. M., Ishai, R., & McKenna, M. J. (2018). Otosclerosis: Temporal bone pathology. *Otolaryngol. Clin. North Am.*, 51(2), 291–303. DOI: 10.1016/j.otc.2017.11.001.
- Wegner, I., Kamalski, D. M., Tange, R. A., Vincent, R., Stegeman, I., van der Heijden, G. J., & Grolman, W. (2014). Laser versus conventional fenestration in stapedotomy for otosclerosis: a systematic review. *Laryngoscope*, 124(7), 1687–1693. DOI: 10.1002/lary.24514.
- Pauli, N., Strömbäck, K., Lundman, L., & Dahlin-Redfors, Y. (2020). Surgical technique in stapedotomy hearing outcome and complications. *The Laryngoscope*, 130, 790–796. DOI: 10.1002/lary.28072.
- Ho, S., Patel, P., Ballard, D., Rosenfeld, R., & Chandrasekhar, S. (2021). Systematic review and meta-analysis of endoscopic vs microscopic stapes sur-

- gery for stapes fixation. *Otolaryngol. Head Neck Surg.*, 165(5), 626–635. DOI: 10.1177/0194599821990669.
7. Bagger-Sjöbäck, D., Strömbäck, K., Hultcrantz, M., Papatziomos, G., Smeds, H., Danckwardt-Lillieström, N., Tideholm, B., Johansson, A., Hellström, S., Hakizimana, P., & Fridberger, A. (2015). High-frequency hearing, tinnitus, and patient satisfaction with stapedotomy: A randomized prospective study. *Sci. Rep.*, 21(5), 13341. DOI: 10.1038/srep13341.
 8. Roychowdhury, P., Polanik, M. D., Kempfle, J. S., Castillo-Bustamante, M., Fikucki, C., Wang, M. J., Kozin, E. D., & Remenschneider, A. K. (2021). Does stapedotomy improve high frequency conductive hearing? *Laryngoscope Investig. Otolaryngol.*, 6(4), 824–831. DOI: 10.1002/lio2.599.
 9. Ramaswamy, A. T., & Lustig, L. R. (2018). Revision surgery for otosclerosis. *Otolaryngol. Clin. North Am.*, 51(2), 463–474. DOI: 10.1016/j.otc.2017.11.014.
 10. Lundman, L., Strömbäck, K., Björnsne, A., Grendin, J., & Dahlin-Redfors, Y. (2020). Otosclerosis revision surgery in Sweden: hearing outcome, predictive factors and complications. *Eur. Arch. Otorhinolaryngol.*, 277(1), 19–29. DOI: 10.1007/s00405-019-05652-w.
 11. Ramaswamy, A. T., & Lustig, L. R. (2018). Revision surgery for otosclerosis. *Otolaryngol. Clin. North Am.*, 51(2), 463–474. DOI: 10.1016/j.otc.2017.11.014.
 12. Kwacz, M., Rymuza, Z., Michałowski, M., & Wysocki, J. (2015) Elastic properties of the annular ligament of the human stapes-AFM measurement. *J. Assoc. Res. Otolaryngol.*, 16(4), 433–446. DOI: 10.1007/s10162-015-0525-9.
 13. International Organization for Standardization. (2018). Biological evaluation of medical devices – Part 1: Evaluation and testing within a risk management process. ISO 10993-1:2018.
 14. Laverty, G., & Gilmore, B. (2012). Characteristics and treatment of medical device related infections. In *Advances in medicine and biology* (Vol. 51, pp. 79–140). Nova Publishers.
 15. International Organization for Standardization. (2013). Non-active surgical implants – General requirements. ISO 14630:2013.
 16. Lerouge, S. (2012). Introduction to sterilization: Definitions and challenges. In *Sterilization of biomaterials and medical devices* (pp. 1–19). Sawston, UK: Woodhead Publishing.
 17. Tipnis, N. P., & Burgess, D. J. (2018). Sterilization of implantable polymer-based medical devices: A review. *Int. J. Pharm.*, 544(2), 455–460. DOI: 10.1016/j.ijpharm.2017.12.003.
 18. Galante, R., Pinto, T. J. A., Colaço, R., & Serro, A. P. (2018). Sterilization of hydrogels for biomedical applications: A review. *J. Biomed. Mater. Res. B Appl. Biomater.*, 106(6), 2472–2492. DOI: 10.1002/jbm.b.34048.
 19. Münker, T. J. A. G., van de Vijfeijken, S. E. C. M., Mulder, C. S., Vespasiano, V., Becking, A. G., Kleverlaan, C. J., CranioSafe Group, CranioSafe Group, Becking, A. G., Dubois, L., Karssemakers, L. H. E., Milstein, D. M. J., van de Vijfeijken, S. E. C. M., Depauw, P. R. A. M., Hoefnagels, F. W. A., Vandertop, W. P., Kleverlaan, C. J., Münker, T. J. A. G., Maal, T. J. J., Nout, E., Riool, M., & Zaat, S. A. J. (2018). Effects of sterilization on the mechanical properties of poly(methyl methacrylate) based personalized medical devices. *J. Mech. Behav. Biomed. Mater.*, 81, 168–172. DOI: 10.1016/j.jmbbm.2018.01.033.
 20. Shintani, H. (2017). Ethylene oxide gas sterilization of medical devices. *Biocontrol. Sci.*, 22(1), 1–16. DOI: 10.4265/bio.22.1.
 21. Stoppel, W. L., White, J. C., Horava, S. D., Henry, A. C., Roberts, S. C., & Bhatia, S. R. (2014). Terminal sterilization of alginate hydrogels: efficacy and impact on mechanical properties. *J. Biomed. Mater. Res. B Appl. Biomater.*, 102(4), 877–884. DOI: 10.1002/jbm.b.33070.
 22. Ashfaq, A., Clochard, M. C., Coqueret, X., Dispenza, C., Driscoll, M. S., Ulański, P., & Al-Sheikhly, M. (2020). Polymerization reactions and modifications of polymers by ionizing radiation. *Polymers (Basel)*, 30(12), 2877. DOI: 10.3390/polym12122877.
 23. Singh, R., Singh, D., & Singh, A. (2016). Radiation sterilization of tissue allografts: A review. *World J. Radiol.*, 8(4), 355–369. DOI: 10.4329/wjr.v8.i4.355.
 24. International Organization for Standardization. (2020). Biological evaluation of medical devices – Part 18: Chemical characterization of materials. ISO 10993-18:2020.
 25. Hasanain, F., Guenther, K., Mullett, W. M., & Craven, E. (2014). Gamma sterilization of pharmaceuticals – a review of the irradiation of excipients, active pharmaceutical ingredients, and final drug product formulations. *PDA J. Pharm. Sci. Technol.*, 68(2), 113–137. DOI: 10.5731/pdajpst.2014.00955.
 26. International Organization for Standardization. (2006). Sterilization of health care products – Radiation Part 1: Requirements for development, validation and routine control of a sterilization process for medical devices. ISO 11137-1:2006.
 27. Zhao, Y., Zhu, B., Wang, Y., Liu, Ch., & Shen, Ch. (2019) Effect of different sterilization methods on the properties of commercial biodegradable polyesters for single-use, disposable medical devices. *Mater. Sci. Eng. C*, 105, 110041. DOI: 10.1016/j.msec.2019.110041.
 28. Sadlo, J., Strzelczak, G., Lewandowska-Szumiel, M., Sterniczuk, M., Pajchel, L., & Michalik, J. (2012). Carbon-centered radicals in γ -irradiated bone substituting biomaterials based on hydroxyapatite. *J. Mater. Sci. Mater. Med.*, 23, 2061–2068. DOI:10.1007/s10856-012-4680-9.
 29. Bargh, S., Silindir-Gunay, M., Yekta Ozer, A., Palaska, E., Karaarslan, D., Ide, S., & Solpan, D. (2020). Physicochemical evaluation of gamma and microwave irradiated dental grafts. *Radiat. Phys. Chem.*, 170, 108627. DOI: 10.1016/j.radphyschem.2019.108627.
 30. Monaco, G., Cholas, R., Salvatore, L., Madaghiele, M., & Sannino, A. (2016). Sterilization of collagen scaffolds designed for peripheral nerve regeneration: Effect on microstructure, degradation and cellular colonization. *Mater. Sci. Eng. C Mater. Biol. Appl.*, 1(71), 335–344. DOI: 10.1016/j.msec.2016.10.030.
 31. International Organization for Standardization. (2015). Metallic materials – Instrumented indentation test for hardness and materials parameters – Part 1: Test method. ISO 14577-1:2015.
 32. Oliver, W. C., & Pharr, G. M. (1992). An improved technique for determining hardness and elastic modu-

- lus using load and displacement sensing indentation experiments. *J. Mater. Res.*, 7(6), 1564–1583.
33. Oliver, W. C., & Pharr, G. M. (2004). Measurement of hardness and elastic modulus by instrumented indentation: Advances in understanding and refinements to methodology. *J. Mater. Res.*, 19, 3–20. DOI: 10.1557/jmr.2004.19.1.3.
 34. Ekwińska, M., & Rymuza, Z. (2009). Normal force calibration method used for calibration of atomic force microscope. *Acta Phys. Pol. A*, 116, S78–S81.
 35. International Organization for Standardization. (2009). Biological evaluation of medical devices – Part 5: Tests for in vitro cytotoxicity. ISO 10993-5:2009.
 36. El Fray, M., Przybytniak, G., Piątek-Hnat, M., & Kornacka, E. M. (2010). Physical effects of radiation processes in poly(aliphatic/aromatic-ester)s modified with e-beam radiation. *Polymer*, 51(5), 1133–1139. DOI: 10.1016/j.polymer.2010.01.028.
 37. Walo, M., Przybytniak, G., Nowicki, A., & Świeszkowski, W. (2011). Radiation-induced effects in gamma-irradiated PLLA and PCL at ambient and dry ice temperatures. *J. Appl. Polym. Sci.*, 122(1), 375–383. DOI: 10.1002/app.34079.
 38. Walo, M., Przybytniak, G., Łyczko, K., & Piątek-Hnat, M. (2013). The effect of hard/soft segment composition on radiation stability of poly(ester-urethane)s. *Radiat. Phys. Chem.*, 94, 18–21. DOI: 10.1016/j.radphyschem.2013.06.014.
 39. Lamblin, G., Leprince, J., Devaux, J., Mestdagh, M., Gallez, B., & Leloup, G. (2010). Hydroxyl radical release from dental resins: Electron paramagnetic resonance evidence. *Acta Biomater.*, 6(8), 3193–3198. DOI: 10.1016/j.actbio.2010.03.001.
 40. Pudlik, M. (2020). *Optimization of the chamber stapes prosthesis manufacturing process*. Unpublished doctoral dissertation, Warsaw University of Technology, Warsaw, Poland.
 41. Greenwood, J. A., & Williamson, J. B. P. (1966). Contact of nominally flat surfaces. *Proc. R. Soc. Lond. A*, 295(1442), 300–319.
 42. Greenwood, J. A., & Tripp, J. H. (1971). The contact of two nominally rough surfaces. *Proc. Inst. Mech. Eng.*, 185, 625–633.
 43. Manas, D., Ovsik, M., Mizera, A., Manas, M., Hyllova, L., Bednarik, M., & Stanek, M. (2018). The effect of irradiation on mechanical and thermal properties of selected types of polymers. *Polymers*, 10, 158. DOI: 10.3390/polym10020158.
 44. Banasik, K., & Kwacz, M. (2017). Numerical study of the PDMS membrane designed for new chamber stapes prosthesis. In R. Jabłoński & R. Szewczyk (Eds.), *Recent global research and education: Technological challenges*. (Advances in Intelligent Systems and Computing, vol. 519, pp. 223–228). Springer, Cham. DOI: 10.1007/978-3-319-46490-9_32.
 45. Cho, K., Rajan, G., Farrar, P., Prentice, L., & Gangadhara Prusty, B. (2022). Dental resin composites: A review on materials to product realizations. *Compos. Pt. B-Eng.*, 230, 109495, DOI: 10.1016/j.compositesb.2021.109495.
 46. Cramer, N. B., Stansbury, J. W., & Bowman, C. N. (2011). Recent advances and developments in composite dental restorative materials. *J. Dent. Res.*, 90(4), 402–416. DOI: 10.1177/0022034510381263.
 47. Shiraiishi, K., & Yokoyama, M. (2019). Toxicity and immunogenicity concerns related to PEGylated-micelle carrier systems: a review. *Sci. Technol. Adv. Mater.*, 20(1), 324–336. DOI: 10.1080/14686996.2019.1590126.
 48. Tamura, A., Fukumoto, I., Yui, N., Matsumura, M., & Miura, H. (2015). Increasing the repeating units of ethylene glycol-based dimethacrylates directed toward reduced oxidative stress and co-stimulatory factors expression in human monocytic cells. *J. Biomed. Mater. Res. A*, 103(3), 1060–1066. DOI: 10.1002/jbm.a.35251.
 49. Hu, W., Ying, M., Zhang, S., & Wang, J. (2018). Poly(amino acid)-based carrier for drug delivery systems. *J. Biomed. Nanotechnol.*, 14(8), 1359–1374. DOI: 10.1166/jbn.2018.2590.
 50. Spicer, C. D. (2020). Hydrogel scaffolds for tissue engineering: the importance of polymer choice. *Polym. Chem.*, 11(2), 184–219. DOI: 10.1039/C9PY01021A.
 51. Lin, H. R., Wang, S. H., Chiang, C. C., Juang, Y. C., Yu, F. A., & Tsai, L. (2015). High strain-rate response of injectable PAA hydrogel. *J. Biomater. Sci.-Polym. Ed.*, 26(9), 534–544. DOI: 10.1080/09205063.2015.1034598.
 52. Cui, L. -Y., Cheng, S. -C., Liang, L. -X., Zhang, J. -C., Li, S. -Q., Wang, Z. -L., & Zeng, R. -C. (2020). In vitro corrosion resistance of layer-by-layer assembled polyacrylic acid multilayers induced Ca-P coating on magnesium alloy AZ31. *Bioact. Mater.*, 5(1). DOI: 10.1016/j.bioactmat.2020.02.001.
 53. Browe, D. P., Wood, C., Sze, M. T., White, K. A., Scott, T., Olabisi, R. M., & Freeman, J. W. (2017). Characterization and optimization of actuating poly(ethylene glycol) diacrylate/acrylic acid hydrogels as artificial muscles. *Polymer (Guildf)*, 19(117), 331–341. DOI: 10.1016/j.polymer.2017.04.044.